Sparse Kernel Affine Projection-Based Nonlinear Distortion Compensation and Memory Effect Depression Algorithm in VLC Systems

Jieling Wang 🔗, Ni Chen 🔗, Shurong Zhang 🔗, *Member, IEEE*, and Mao Zhao

Abstract—As an emerging wireless application for indoor high-speed wireless access and positioning, visible light communication (VLC) has attracted people's attentions. However, the nonlinear components employed in VLC systems, especially the light-emitting diodes (LEDs), can cause nonlinear distortion to the transmitted signal, which could severely degrade the system performance. Aiming at the nonlinear characteristics of LED, the sparse kernel affine projection algorithm (SKAPA) is investigated in this paper to eliminate the nonlinear distortion for VLC systems. Based on that, to further remove the bad memory effect of LED, a memory effect depression (MED) scheme is proposed, which is carried out following SKAPA. Simulation results show that SKAPA can compensate for the nonlinear distortions, and the combined SKAPA-MED algorithm has a good performance in dealing with memory LEDs. Compared with Kernel Least-Mean-Square (KLMS), SKAPA exhibits better convergence and bit error rate (BER) performance. Additionally, it is also demonstrated that SKAPA has lower complexity than memory polynomial algorithm, and slightly better detection property can be obtained.

Index Terms—Memory effect, nonlinear distortion, sparse kernel affine projection algorithm, visible light communication.

I. INTRODUCTION

WITH the ever increasing transmission data rate in wireless communications, spectrum resources in radio frequency (RF) are becoming increasingly scarce, thus finding new communication bands has been one of the research hotspots in academia. Due to the stable operating principle of light-emitting diode (LED), LED devices have been widely deployed, and the research of visible light communication (VLC) technology has found wide applications, which can help address the challenges faced by RF communications, such as energy efficiency, bandwidth limitation, electromagnetic radiation and safety *et al.* [1].

Nonlinearity, which has been one of the important problems in RF systems, is still a threat to VLC systems, since nonlinear devices are also employed. Nonlinear effect may come from digital-to-analog converter (DAC), driving circuits of the LED, LED, photodiodes (PDs) and analog-to-digital converter (ADC), among which LED dominates the main nonlinearity [1]. Specifically speaking, electro-optical conversion of LED is the most important source of nonlinearity in VLC systems, while by contrast, the nonlinearity caused by PD photoelectric conversion can be ignored [2]. Intensity modulation direct detection (IM/DD) technique is usually employed at the optical front-end, which could make the VLC systems performance susceptible to nonlinearity. Compared with the orthogonal frequency division multiplexing (OFDM) in RF systems, the peak to average power ratio (PAPR) of the optical OFDM (O-OFDM) signal is even higher [3], so the modulation adopted by VLC systems is also sensitive to nonlinearity.

Digital predistortion (DPD) is one of the popular methods to mitigate the nonlinear impact of LED. The linearization technique uses digital filter with inverse response to the LED response, so that the cascade of DPD and LED present a linear input-output relationship [4], which could be accomplished by direct learning [5], [6] and indirect learning architectures [7], [8]. In [5], a DPD scheme is proposed to lighten the LED nonlinearity, which greatly enhances the system performance. To precisely estimate the nonlinear characteristics of LED, the Chebyshev nonlinear mapping is adopted to process the signal before transmitted to predistorter [6]. The memoryless power series based on adaptive predistortion method is utilized to decline nonlinear impairments of high-speed VLC system [7]. Adaptive learning architecture in [8] can track the dynamic changes of LED and achieve superior system performance.

As an essential part of DPD, physical sampling and feedback circuits are needed at the transmitter, which could be cost-inefficient under some scenarios, so people developed the postdistortion techniques at the receiver side. For VLC, postdistortion is more suitable to follow the dynamic nonlinearity depending on the conditions of aging and heating effect of LED, and meanwhile, it allows for no precise approximation of LED characteristics. The second-order Volterra series model is exploited in [9] to construct a DFE which attains an evident performance gain. In [10], two solutions of inverse LED nonlinear characteristic are given with training sequence by minimizing the power of error signal. Wang *et al.* accomplish a

high transmission rate based on high-speed carrierless amplitude and phase modulation [11], and subsequently, they propose a hybrid post equalizer, which includes a Volterra series nonlinear equalizer and a decision-directed least mean square (LMS) equalizer [12]. Sparse Bayesian learning and Kalman filtering are combined in [13] to extract the active Volterra series kernels decreasing the redundancy of postdistortion equalizer.

The PAPR reduction techniques are also considered for the nonlinearity removal in VLC systems, such as clipping [14], [15], companding technique [16], [17], and precoder [18], [19]. In [14], a low complexity detector is provided to process the clipped signal using maximum likelihood sequence detection criterion. The authors in [15] advance an adaptive symbol decomposition scheme in serial transmissions. The μ-law companding technique is introduced into VLC system [16], and in [17], three types of piecewise companding devices are utilized to lessen the clipping distortion of high-peak signal. The output signal of one-bit sigma-delta modulator designed in [18] is transformed to be ON-OFF keying signal, and Hadamard coded modulation technique draws on fast Walsh-Hadamard transform instead of OFDM to modulate the signal [19], both of which can diminish the nonlinear effect of systems.

Kernel adaptive filtering (KAF) technology based on reproducing kernel Hilbert space (RKHS) maps nonlinear problems into linear problems with high-dimensional feature space, and then makes use of kernel techniques to convert complex operations in the feature space into low-dimensional kernel function calculations [20]. With further research on KAF technology, it has been applied to VLC systems to ease nonlinear impact, specifically as kernel minimum symbol error rate (KMSER) [21], [22], kernel RLS (KRLS) [23], [24] and Kernel LMS (KLMS) [25], [26]. KMSER equalizer can reduce the computational complexity while ensuring system performance using sparse technique [21], and the concept of hybrid kernel adaptive learning mechanism is presented in [22], which has a rapid convergence. KRLS algorithm utilizing random Fourier features (RFF) and KMSER-RFF algorithm is suggested in [23] to constrict nonlinear distortion of signal, which is improved with decision feedback mechanism in [24]. RFF-KLMS is advised to alleviate LED's nonlinearity, which does not require sparsification [25]. Multivariate KLMS algorithm incorporated with novelty criterion (NC) sparsification is provided for restriction of Red-Green-Blue LED's nonlinear distortions [26].

Kernel affine projection algorithm (KAPA) appears as an intermediate complexity algorithm between KLMS and KRLS, which inherits the simplicity of KLMS while reducing the gradient noise by using multiple samples. As an interesting method, KAPA has been exploited in optical fiber communication to eliminate the nonlinear impairments [27]. Three variants of KAPA are proposed in [27], and the experimental results show that KAPA can effectively remove nonlinear impairments in short reach communication while maintaining low complexity in RKHS.

In this paper, focusing on the characteristics of VLC systems, we study KAPA with NC based sparsification, which is referred to as SKAPA. Then, we apply it to compensate for the nonlinear distortion in VLC systems, and the memory effect depression (MED) algorithm is designed to mitigate the memory effect

impacts of LED modeled by Wiener model. Simulation results are presented to show the effectiveness of the SKAPA-MED algorithm with bit error rate (BER) performance.

II. SYSTEM MODEL

The block diagram of baseband transmission system model is shown in Fig. 1, which utilizes direct current biased O-OFDM (DCO-OFDM) modulation technique. Frequency domain signal vector $\bar{\mathbf{X}} = [\bar{X}(1), \ldots, \bar{X}(k), \ldots, \bar{X}(N/2 - 1)]$ is obtained by QAM mapping, where N is the number of subcarriers. To meet the requirement that the driving signal of LED must be a real value, the signal $\bar{\mathbf{X}}$ is modulated onto N subcarriers through the Hermitian symmetry as

$$X(k) = \begin{cases} 0, & k = 0, N/2 \\ \bar{X}(k), & k = 1, 2, \ldots, N/2 - 1 \\ \bar{X}^*(N - k), & k = N/2 + 1, \ldots, N - 1 \end{cases} \quad (1)$$

where $\bar{X}(k)$ and $\bar{X}^*(k)$ are conjugate symmetry, hence the DCO-OFDM signal vector $\mathbf{X} = [0, \bar{\mathbf{X}}, 0, \bar{\mathbf{X}}^*]$ is constructed. The real-valued time domain signal vector $\mathbf{x} = [x(0), \ldots, x(n), \ldots, x(N - 1)]$ is then attained with inverse fast Fourier transform (IFFT) operation.

In order to realize the non-negativity of the driving signal, the DC bias v_{dc} is added to $x(n)$ before being fed to LED, where $v_{dc} = \mu\sqrt{E\{x^2(n)\}}$, μ is a positive scale factor, and $E(\cdot)$ means expectation.

Next, the drive signal $x_{dc}(n)$ with DC bias is sent to LED. The nonlinearity and memory effect of LED are described by Wiener model illustrated in Fig. 2, which consists of a linear time-invariant (LTI) block and a nonlinear (NL) block. The LTI block is expressed as

$$r(n) = \sum_{m=0}^{M-1} b_m x_{dc}(n - m) \quad (2)$$

where M represents memory depth and b_m is the coefficient. The NL block can be explained with a Rapps model [10] as

$$z(n) = \begin{cases} \dfrac{(r(n) - \mathrm{V}_{on})}{\left(1 + \left(\frac{r(n) - \mathrm{V}_{on}}{I_{\max}}\right)^{2k}\right)^{1/2k}}, & r(n) \geq \mathrm{V}_{on} \\ 0, & r(n) < \mathrm{V}_{on} \end{cases} \quad (3)$$

where $\mathrm{V}_{on}, I_{max},$ and k are threshold voltage, saturation current of LED and knee factor, respectively. Fig. 3(a) shows the nonlinear characteristics when knee factor k is 2, and threshold voltage V_{on} is 0.2 V, from which we can clearly see the nonlinearity. Fig. 3(b) shows the frequency response of LED, which exhibits obvious memory effect due to unevenness of the frequency response.

Considering the light source distribution model of LED and line of sight of transmission path, assuming that the conversion factor of PD is 1, and ignoring the gain of optical filter, the channel gain [25] can be given as

$$h = \begin{cases} \dfrac{S_{PD}(l+1)}{2\pi d^2} \cos^l(\phi)\cos(\varphi), & 0 \leq \varphi \leq \Phi \\ 0, & \varphi > \Phi \end{cases} \quad (4)$$

where S_{PD} is the effective collection area of PD, d is the distance between LED and PD, φ is the incident angle of PD, Φ is the field of view of PD, ϕ is the emission angle of LED, and Lambert
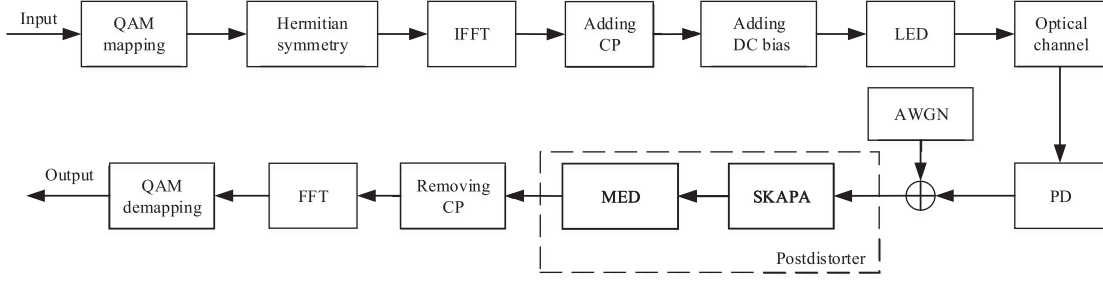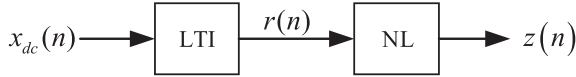
Fig. 1. System model.

Fig. 2. Wiener model.

radiation coefficient $l = -1/(\log_2 \cos(\Psi_{1/2}))$ is determined by the half power angle $\Psi_{1/2}$ of LED.

The received signal can be expressed as follows

$$\hat{y}(n) = h \cdot f\left(x_{dc}(n)\right) + v(n) \qquad (5)$$

where $f(\cdot)$ signifies the input and output function of LED including memory effect and nonlinear characteristics, and $v(n)$ is additive white Gaussian noise. The result of $\hat{y}(n)$ equalized by h, $y(n)$, is applied as an input to the proposed SKAPA-MED postdistorter to recover the transmitted signal.

III. NONLINEAR POSTDISTORTION COMPENSATION

A. SKAPA

In this section, SKAPA is used to mitigate the nonlinear distortion. Let $\mathbf{d}$ and $\mathbf{z}$ be the expected signal vector and the distorted signal vector. $\varphi(\mathbf{z}(i))$ can be obtained, denoted as $\varphi_{\mathbf{z}}(i)$, after transforming $\mathbf{z}(i)$ into a high-dimensional feature space employed by kernel-induced mapping [20]. The weight vector $\boldsymbol{\omega}$ obtained by solving $\min \mathbf{E}|d - \boldsymbol{\omega}^T \varphi_{\mathbf{z}}(i)|^2$ based on the K nearest observations and input values is written as follows

$$\boldsymbol{\omega}(i) = \boldsymbol{\omega}(i-1) + \eta \boldsymbol{\Phi}_{\mathbf{z}}(i) \left[\boldsymbol{\Phi}_{\mathbf{z}}(i)^T \boldsymbol{\Phi}_{\mathbf{z}}(i) + \varepsilon \mathbf{I}\right]^{-1} \mathbf{e}_{\mathbf{z}}(i) \quad (6)$$

where η is the step-size parameter, ε is a small positive smoothing factor, $\boldsymbol{\Phi}_{\mathbf{z}}(i) = [\varphi_{\mathbf{z}}(i-K+1), \ldots, \varphi_{\mathbf{z}}(i)]$, and $\mathbf{e}_{\mathbf{z}}(i) = \mathbf{d}(i) - \boldsymbol{\Phi}_{\mathbf{z}}(i)^T \boldsymbol{\omega}(i-1)$.

Let $\mathbf{G}^{-1} = [\boldsymbol{\Phi}_{\mathbf{z}}(i)^T \boldsymbol{\Phi}_{\mathbf{z}}(i) + \varepsilon \mathbf{I}]^{-1}$, after series simplification as is described in [20], we can have

$$\boldsymbol{\omega}(i) = \boldsymbol{\omega}(i-1) + \eta \boldsymbol{\Phi}_{\mathbf{z}}(i) \mathbf{G}^{-1} \mathbf{e}_{\mathbf{z}}(i)$$

$$= \sum_{n=1}^{i-1} \mathbf{a}_n(i-1)\varphi_{\mathbf{z}}(n) + \mathbf{G}^{-1} \sum_{n=1}^{K} \eta \mathbf{e}_{\mathbf{z}n}(i)\varphi_{\mathbf{z}}(i+K-n) \tag{7}$$

where the expansion coefficients $\mathbf{a}_n(i)$ can be classified as (2), and $\kappa(\mathbf{z}(n), \mathbf{z}(i))$, symbolized as $\kappa_{n,i}$ is a continuous, symmetric, positive-definite kernel function.

Conveniently, the prediction error $e_{\mathbf{z}}(i; k)$ is applied to replace $d(k) - \sum_{n=1}^{i-1} \mathbf{a}_n(i-1)\kappa_{n,k}$ in (8) shown as the bottom of this page, and if g_i is used to stand for the estimate of input-output mapping at time i, the sequential learning rule for KAPA can be written as follows

$$g_i = g_{i-1} + \eta \mathbf{G}^{-1} \sum_{n=i-K+1}^{i} e_{\mathbf{z}}(i; n)\kappa(\mathbf{z}(n), \cdot). \tag{9}$$

Online NC sparsification is employed to remove redundant data and decrease the size of dictionary C. The specific process of SKAPA is shown in Algorithm I.

B. Memory Effect Depression Algorithm

In this subsection, the memory effect depression (MED) algorithm following SKAPA is proposed to solve the residual distortion caused by memory effect of LED. (3) can be expressed in matrix form as

$$\mathbf{r} = \mathbf{b}\mathbf{x}_{dc}. \tag{10}$$

Considering the procedure of adding CP in OFDM system, where $\mathbf{b}$ can actually be equivalent to a $N \times N$ cyclic matrix

$$\mathbf{a}_k(i) = \begin{cases} \eta \mathbf{G}^{-1} \left(d(i) - \sum_{n=1}^{i-1} \mathbf{a}_n(i-1)\kappa_{n,k}\right), & k = i \\ \mathbf{a}_k(i-1) + \eta \mathbf{G}^{-1} \\ \left(d(k) - \sum_{n=1}^{i-1} \mathbf{a}_n(i-1)\kappa_{n,k}\right), & i-K+1 \leq k \leq i-1 \\ \mathbf{a}_k(i-1), & 1 \leq k < i-K+1 \end{cases} \tag{8}$$
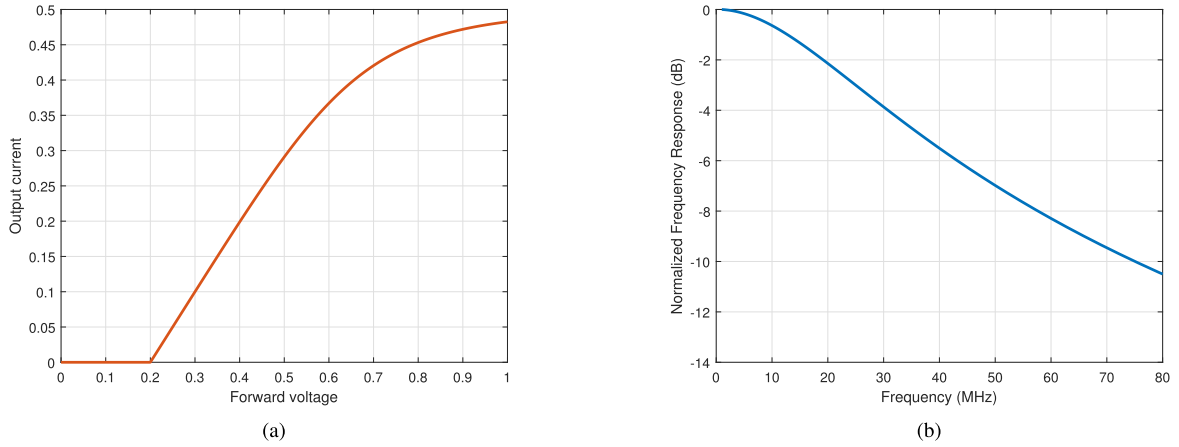
Fig. 3.   Characteristics of LED. (a) LED Nonlinear transfer characteristics modelled by Rapps. (b) Frequency response of Wiener model.

with the elements $[b_0, 0, \ldots, 0, b_{M-1}, \ldots, b_2, b_1]$ of the first row.

$$\mathbf{b} = \begin{bmatrix} b_0 & 0 & \cdots & 0 & b_{M-1} & \cdots \\ \vdots & b_0 & 0 & \cdots & 0 & b_{M-1} \\ b_{M-1} & \cdots & b_0 & 0 & \cdots & 0 \\ 0 & b_{M-1} & \cdots & \ddots & \ddots & \vdots \\ \vdots & \vdots & b_{M-1} & \cdots & \ddots & 0 \\ 0 & \cdots & 0 & b_{M-1} & \cdots & b_0 \end{bmatrix}. \quad (11)$$

The key to removing the memory effect lies in the solution of the filter coefficients matrix $\mathbf{b}$. When a low-power signal is input to LED, it will fall in the linear working area of LED, which can be considered unaffected by the LED's nonlinearity, but it will still be involved by the memory effect. Therefore if the low-power input signal and output signal of LED are known at the receiver-side, namely $\mathbf{x}_{dc}$ and $\mathbf{r}$ in (10), $\mathbf{b}$ can be estimated in the frequency domain.

Denote $\mathbf{X}_{dc}$ and $\hat{\mathbf{R}}$ as the results obtained by performing FFT operations on the low-power $\mathbf{x}_{dc}$ and the corresponding received signal $\hat{\mathbf{r}}$ respectively, and the frequency domain filter coefficients can be gained by the following formula

$$\mathbf{\Lambda} = \frac{\hat{\mathbf{R}}}{\mathbf{X}_{dc}}. \quad (12)$$

Consequently, the estimated filter coefficients matrix $\hat{\mathbf{b}}$ is constructed by $\hat{b}_0, \hat{b}_1 \ldots, \hat{b}_{M-1}$ which come from performing IFFT operation on $\mathbf{\Lambda}$, so that the memory effect distortion compensation processing of the signal can be realized. It is worth noting that since the FFT operation here inevitably changes the symmetry of signal spectrum, setting the specific position of $\mathbf{\Lambda}$ as zero is necessary, which is similar to (1).

IV. SIMULATIONS

The performance of the proposed SKAPA-MED algorithm is tested by Monte Carlo simulations, where the O-OFDM signal using 16-QAM modulation with 1024 subcarriers is considered. The symbol rate is fixed at 10 Ksps, so the bandwidth of OFDM

Algorithm 1: SKAPA.

Require:
   step-size parameter η, kernel function κ and corresponding kernel parameter, number of observations K, smoothing factor ε, sparse threshold ε_d and ε_e, dictionary $C(1) = \{\mathbf{z}(1)\}$, $\mathbf{a}_1(1) = \eta d(1)$

Ensure:
   %(1)Sparsification
1: **if** $\min_{\mathbf{c}_n \in C(i-1)} \|\mathbf{c}_n - \mathbf{z}(i)\| < \varepsilon_d$ **then**
2:     $C(i) = \{C(i-1)\}$
3:     continue
4: **end if**
5: $\mathbf{a}_i(i-1) = 0$
6: $\mathbf{y}(i;k) = \sum_{n=1}^{i-1} \mathbf{a}_n(i-1)\kappa_{n,k}$
7: $e_{\mathbf{z}}(i;k) = d(k) - \mathbf{y}(i;k)$
8: **if** $|e_{\mathbf{z}}(i;k)| < \varepsilon_e$ **then**
9:     $C(i) = \{C(i-1)\}$
10:    continue
11: **else**
12:    $C(i) = \{C(i-1), \mathbf{z}(i)\}$
13: **end if**
   %(2)KAPA Equalization
14: **for** $k \in [\max(1, i-K+1), i]$ **do**
15:    $\mathbf{y}(i;k) = \sum_{n=1}^{i-1} \mathbf{a}_n(i-1)\kappa_{n,k}$
16:    $e_{\mathbf{z}}(i;k) = d(k) - \mathbf{y}(i;k)$
17:    $\mathbf{a}_k(i) = \mathbf{a}_k(i-1) + \eta \mathbf{G}^{-1} e_{\mathbf{z}}(i;k)$
18: **end for**
19: **if** $i > K$ **then**
20:    **for** $k \in [1, i-K]$ **do**
21:       $\mathbf{a}_k(i) = \mathbf{a}_k(i-1)$
22:    **end for**
23: **end if**

---

signal is 10.24MHz. Since only 511 subcarriers can be employed to transmit the information for the adoption of Hermitian symmetry processing, the data rate is 20.44Mbps. The cyclic prefix length is 64, which means that the spectral efficiency
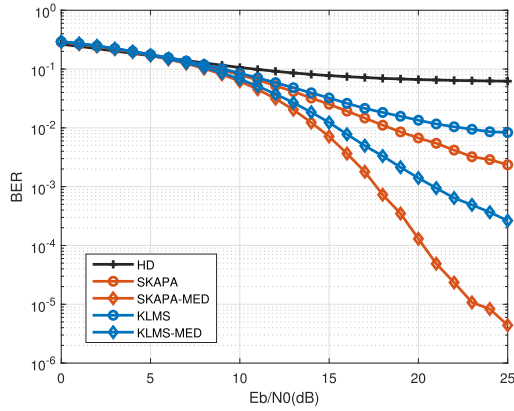
Fig. 4. BER performance curves.

Fig. 5. MSE performance curves with different step sizes.

is $1024/(1024 + 64) = 94.1\%$, so the equivalent bandwidth of OFDM signal is 10.88MHz. The scale factor μ is picked as 4, the I_{max} is chosen as 0.5A, the V_{on} is 0.2 V. The memory depth of the LTI block in Wiener model is set to be 3, the corresponding filter coefficients are 1, 0.15 and 0.1, respectively, and the value of k in the NL block is elected to 2. In the channel model, the S_{PD} is 1 cm^2, the $\Psi_{1/2}$ is picked as $\pi/4$, the ϕ and φ are both $0°$, and the d is 3m. In SKAPA, the Gaussian kernel function is selected, where the kernel parameter a is 20, the thresholds ε_d and ε_e are 0.1 and 0.005. The K is 10, the η is 0.1, and the smoothing factor ε is 0.01.

When power back-off (BO) is 4 dB, that is, the corresponding modulation index is 72%, and the BER performance curves under different signal-to-noise ratios are exhibited in Fig. 4. The modulation index is defined as $MI = \frac{P_{max} - P_{min}}{P_{MAX}}$, where P_{max} and P_{min} are maximum and minimum transmitted power, and P_{MAX} is the maximum rated power [28]. Here, the KLMS also selects Gaussian kernel whose kernel parameter is 60 and step size is set to 0.4. "Slicer" in Fig. 4 stands for the performance of conventional linear reception, and "SKAPA" and "KLMS" denote the performances with postdistorter of SKAPA and KLMS, and "SKAPA-MED" and "KLMS-MED" add an addition MED algorithm to "SKAPA" and "KLMS". It is clear that the performance without postdistortion is poor, and compared to KLMS, SKAPA can achieve a better nonlinear distortion compensation effect. Taking the BER of 2×10^{-3} as an example, SKAPA requires the E_b/N_0 of 25 dB whereas the E_b/N_0 of SKAPA-MED is only 17 dB, which can prove the effectiveness of the MED algorithm, and the same effect can also be seen from the KLMS and KLMS-MED.

The influence of the step size η on the MSE performance is studied and displayed in Fig. 5, where E_b/N_0 is 15 dB, and the BO is 6 dB, and the kernel parameter value is 20. The η of SKAPA are 0.01, 0.05, and 0.1, and the step size values of KLMS algorithm are 0.1 and 0.4. It is clear that SKAPA has faster convergence speed and lower MSE property than KLMS, and when the step size increases, the convergence speed of both algorithms gets faster. But it should be noted that the BER performance of SKAPA will decrease, when the value of η is set to be too large.
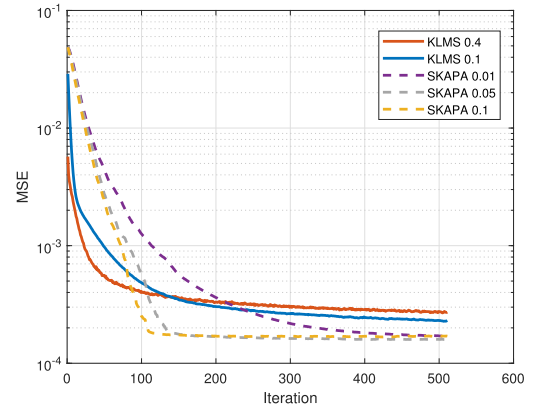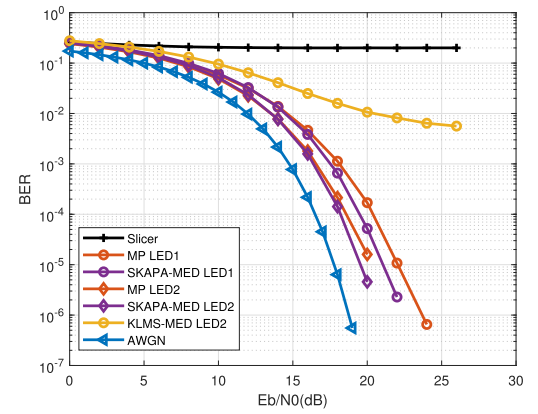

Fig. 6. Performance comparisons of SKAPA, KLMS, and MP.

To further illustrate the effectiveness of the proposed scheme, we compare SKAPA with MP postdistorter in terms of BER properties and computational complexities [10]. In Fig. 6, the performances are tested in DCO-OFDM system with 64 QAM modulation at 10 dB power back-off, where the symbol rate and data rate are fixed at 10 Ksps and 30.66 Mbps respectively, and MI is 28%. "LED1" indicates that the Rapps parameter k is 3, and filter coefficients are 1, 0.3 and 0.1, and "LED2" represents Wiener model with parameter k of 2, filter coefficients of 1, 0.15 and 0.1. As is shown in Fig. 6, we can see that SKAPA algorithm has better performance than MP, where the polynomial order and memory depth of MP are fixed at 7 and 3.

The computational complexities of SKAPA and MP under different FFT sizes are depicted in Fig. 7, where "Q" is the polynomial order and "D" is the memory depth. The complexity of MP depends on FFT size, and increases linearly with the increase of FFT size, whereas the computation complexity of SKAPA is independent of the FFT size, only related to the dictionary C. The dictionary size is relevant to the parameters, such as ε_d and ε_e, so we present the complexities of the commonly-used upper and lower limits of network size. The "SKAPA-LOW" means the computations when network size is 70, and "SKAPA-HIGH" denotes the one with network size being 200. From Fig. 7, it can be concluded that when FFT size is large to a certain extent, the computational complexity of SKAPA is lower than MP.
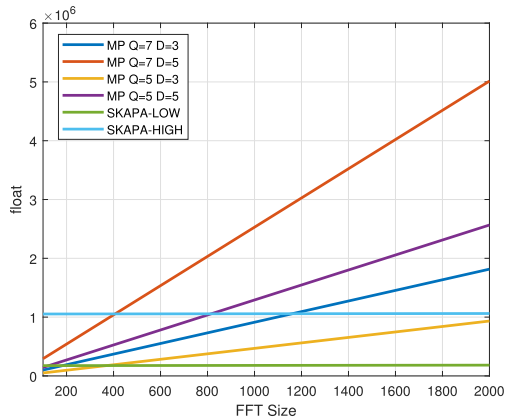
Fig. 7.   Computational complexity against FFT size.

V. CONCLUSION

This paper focuses on the postdistortion compensation technology of the nonlinear signal in VLC systems. The SKAPA is applied to mitigate the nonlinear impact, meanwhile, the MED algorithm is proposed to solve the residual distortion caused by memory effect of LED. The effectiveness of the proposed SKAPA-MED algorithm is verified by simulations, where the influence of various parameters on the system performance is analyzed. Numerical results show that the SKAPA-MED scheme with appropriate parameter values can provide superior BER and MSE performance compared to KLMS and MP, and the proposed one needs comparatively lower complexity than MP when FFT size is properly large.

REFERENCES

[1] K. Ying, Z. Yu, R. J. Baxley, H. Qian, G. Chang, and G. T. Zhou, "Nonlinear distortion mitigation in visible light communications," *IEEE Wireless Commun.*, vol. 22, no. 2, pp. 36–45, Apr. 2015.

[2] D. Tsonev, S. Sinanovic, and H. Haas, "Complete modeling of nonlinear distortion in OFDM-based optical wireless communication," *J. Lightw. Technol.*, vol. 31, no. 18, pp. 3064–3076, Sep. 2013.

[3] M. Gao, C. Li, and Z. Xu, "Optimal transmission of VLC system in the presence of led nonlinearity and APD module saturation," *IEEE Photon. J.*, vol. 10, no. 5, Oct. 2018, Art. no. 7907514.

[4] H. Faig, Y. Yoffe, E. Wohlgemuth, and D. Sadot, "Grading optimization for dimensions-reduced orthogonal volterra DPD," *IEEE Photon. J.*, vol. 12, no. 1, Feb. 2020, Art. no. 7200310.

[5] Q. Wang and D. He, "Adaptive digital predistortion implemented by FPGA and soft microprocessor core," in *Proc. IEEE Adv. Inf. Technol., Electron. Automat. Control Conf.*, 2015, pp. 718–721.

[6] R. Mitra and V. Bhatia, "Chebyshev polynomial-based adaptive predistorter for nonlinear LED compensation in VLC," *IEEE Photon. Technol. Lett.*, vol. 28, no. 10, pp. 1053–1056, May 2016.

[7] Y. Zhou, J. Zhang, C. Wang, J. Zhao, and C. Nan, "A novel memoryless power series based adaptive nonlinear pre-distortion scheme in high speed visible light communication," in *Proc. Opt. Fiber Commun. Conf. Exhib.*, 2017, pp. 1–3.

[8] P. Aggarwal, T. Kabra, R. Ahmad, V. A. Bohara, and A. Srivastava, "Adaptive learning architecture-based predistorter for nonlinear VLC system," *Photon. Netw. Commun.*, vol. 38, no. 2, pp. 258–269, Oct. 2019.

[9] G. Stepniak, J. Siuzdak, and P. Zwierko, "Compensation of a VLC phosphorescent white LED nonlinearity by means of Volterra DFE," *IEEE Photon. Technol. Lett.*, vol. 25, no. 16, pp. 1597–1600, Aug. 2013.

[10] H. Qian, S. J. Yao, S. Z. Cai, and T. Zhou, "Adaptive postdistortion for nonlinear LEDs in visible light communications," *IEEE Photon. J.*, vol. 6, no. 4, Aug. 2014, Art. no. 7901508.

[11] Y. Wang, L. Tao, X. Huang, J. Shi, and N. Chi, "Enhanced performance of a high-speed WDM CAP64 VLC system employing Volterra series-based nonlinear equalizer," *IEEE Photon. J.*, vol. 7, no. 3, Jun. 2015, Art. no. 7901907.

[12] Y. Wang, L. Tao, X. Huang, J. Shi, and N. Chi, "8-Gb/s RGBY LED-based WDM VLC system employing high-order CAP modulation and hybrid post equalizer," *IEEE Photon. J.*, vol. 7, no. 6, Dec. 2015, Art. no. 7904507.

[13] P. Miao, G. Chen, X. Wang, Y. Yao, and J. A. Chambers, "Adaptive nonlinear equalization combining sparse Bayesian learning and Kalman filtering for visible light communications," *J. Lightw. Technol.*, vol. 38, no. 24, pp. 6732–6745, Dec. 2020.

[14] J. Tan, Z. Wang, Q. Wang, and L. Dai, "Near-optimal low-complexity sequence detection for clipped DCO-OFDM," *IEEE Photon. Technol. Lett.*, vol. 28, no. 3, pp. 233–236, Feb. 2016.

[15] K. Jia, B. Yang, M. Cao, Y. Lin, S. Li, and L. Hao, "An adaptive symbol decomposition with serial transmission for O-OFDM-based VLC system," *IEEE Commun. Lett.*, vol. 25, no. 3, pp. 916–920, Mar. 2021.

[16] Y. Yang, Z. Zeng, S. Feng, and C. Guo, "A simple OFDM scheme for VLC systems based on μ-law mapping," *IEEE Photon. Technol. Lett.*, vol. 28, no. 6, pp. 641–644, Mar. 2016.

[17] H. Zhang, L. L. Yang, and L. Hanzo, "Piecewise companding transform assisted optical-OFDM systems for indoor visible light communications," *IEEE Access*, vol. 5, pp. 295–311, 2017.

[18] H. Qian, J. Chen, S. Yao, Z. Y. Zhang, H. Zhang, and W. Xu, "One-bit sigma-delta modulator for nonlinear visible light communication systems," *IEEE Photon. Technol. Lett.*, vol. 27, no. 4, pp. 419–422, Feb. 2015.

[19] M. Noshad and M. Brandt-Pearce, "Hadamard coded modulation for visible light communications," *IEEE Trans. Commun.*, vol. 64, no. 3, pp. 1167–1175, Mar. 2016.

[20] W. Liu, J. Prncipe, and S. Haykin, *Kernel Adaptive Filtering: A Comprehensive Introduction*. Hoboken, NJ, USA: Wiley, 2010.

[21] R. Mitra and V. Bhatia, "Adaptive sparse dictionary-based Kernel minimum symbol error rate post-distortion for nonlinear LEDs in visible light communications," *IEEE Photon. J.*, vol. 8, no. 4, Aug. 2016, Art. no. 7905413.

[22] R. Mitra, F. Miramirkhani, V. Bhatia, and M. Uysal, "Mixture-kernel based post-distortion in RKHS for time-varying VLC channels," *IEEE Trans. Veh. Technol.*, vol. 68, no. 2, pp. 1564–1577, Feb. 2019.

[23] R. Mitra, S. Jain, and V. Bhatia, "Least minimum symbol error rate based post-distortion for VLC using random Fourier features," *IEEE Commun. Lett.*, vol. 24, no. 4, pp. 830–834, Apr. 2020.

[24] S. Jain, R. Mitra, and V. Bhatia, "Kernel MSER-DFE based post-distorter for VLC using random Fourier features," *IEEE Trans. Veh. Technol.*, vol. 69, no. 12, pp. 16241–16246, Dec. 2020.

[25] P. K. Anand, S. Jain, R. Mitra, and V. Bhatia, "Random Fourier features based post-distortion for massive-MIMO visible light communication," in *Proc. Int. Conf. Commun., Signal Process., Their Appl.*, 2021, pp. 1–6.

[26] S. Jain, R. Mitra, and V. Bhatia, "Multivariate-KLMS based post-distorter for nonlinear RGB-LEDs for color-shift keying VLC," in *Proc. IEEE 30th Annu. Int. Symp. Pers., Indoor Mobile Radio Commun.*, 2019, pp. 1–6.

[27] L. Zhang *et al.*, "Kernel affine projection for nonlinearity tolerant optical short reach systems," *IEEE Trans. Commun.*, vol. 68, no. 10, pp. 6403–6412, Oct. 2020.

[28] X. Zhang, P. Liu, J. Liu, and S. Liu, "Advanced A-law employing nonlinear distortion reduction in DCO-OFDM systems," in *Proc. IEEE/CIC Int. Conf. Commun. China - Workshops*, 2015, pp. 184–188.